Geomechanics and Engineering, *Vol. 37, No. 2 (2024) 123-133*
https://doi.org/10.12989/gae.2024.37.2.123

Effects of loading frequency and specimen size on the liquefaction resistance of clean sand

Sung-Sik Park[1a], Dong-Eun Lee[2b] and Dong-Kiem-Lam Tran[*1]

[1]Department of Civil Engineering, Kyungpook National University, 80, Daehak-ro Buk-gu, Daegu 41566, Republic of Korea
[2]Department of Architectural Engineering, Kyungpook National University, 80, Daehak-ro Buk-gu, Daegu 41566, Republic of Korea

(*Received December 12, 2023, Revised March 14, 2024, Accepted March 19, 2024*)

Abstract. This study investigates the effects of loading frequency (*f*) and specimen size on the liquefaction resistance of clean sand. A series of cyclic direct simple shear tests were conducted on Jumunjin sand with varying consolidated relative densities (40% and 80%), *f* values (0.05, 0.10, and 0.20 Hz), and diameter to height (*D/H*) ratios (3.63, 3.18, 2.82, and 2.54). The results demonstrated the significant influence of *f* and *D/H* ratio on the number of cycles to liquefaction ($N_{cyc\text{-}liq}$) and the cyclic resistance ratio (CRR_{15}). It was observed that increasing *f* linearly increased $N_{cyc\text{-}liq}$. Increasing the specimen height also led to higher $N_{cyc\text{-}liq}$ values irrespective of the *f* or relative density. Moreover, a positive correlation between CRR_{15} and *f* indicated that higher *f* yielded higher CRR_{15}. This relationship was more pronounced in dense sand than in loose sand. Specimen height also significantly affected CRR_{15}, with increasing the specimen height resulting in higher CRR_{15} values. Furthermore, the effect of *f* on CRR_{15} was less significant compared to the influence of specimen height. The effect of *f* on the normalized cyclic resistance ratio (*NCRR*) was relatively negligible for loose sand but more substantial for dense sand depending on the *D/H* ratio. Data analysis revealed that the *NCRR* generally decreases as the *D/H* ratio increases. An interpolation formula was provided to calculate the *NCRR* based on the *D/H* ratio regardless of the *f* and relative density.

Keywords: liquefaction resistance of sand; loading frequency; specimen height; specimen size ratio

1. Introduction

The liquefaction resistance of clean sand is an important factor to consider in geotechnical engineering design because it can affect the stability of structures built on or near sandy soils. One of the key factors that can affect the liquefaction resistance of sand is the specimen size ratio (*D/H*), which is defined as the ratio of the specimen diameter (*D*) to the specimen height (*H*). The *D/H* ratio can influence the development of stress and strain nonuniformities within the soil mass (Shen *et al.* 1978, Amipour *et al.* 2022), which can affect the liquefaction resistance of sand. Carroll (1979) investigated the effect of *D/H* ratio on the strength and deformation behavior of granular soils by conducting cyclic direct simple shear (CDSS) tests with varying specimen dimensions (D = 47.6 and 80 mm and H = 10, 15, and 25 mm). The study showed that specimen size affected the strength and deformation behavior of granular soils, with smaller specimens displaying greater strength and stiffness. Kovacs and Leo (1981) investigated the influence of *D/H* ratio on the cyclic simple shear behavior of large-scale sand specimens. The study found that a lower *D/H* ratio reduced the number of cycles required to attain a steady-state condition. Larger *D/H* ratios increased pore pressure generation and more significant axial strain accumulation. Chang *et al.* (2016) investigated the effects of specimen size and boundary conditions on the stress–strain behavior of soils using direct simple shear (DSS) tests. Numerical experiments using the distinct element method revealed that specimen size and boundary conditions had significant effects on the stress–strain behavior of the specimen. The effect of boundary conditions was reduced effectively when the *D/H* ratio increased, and there was a relatively consistent stress–strain relationship when the H/d_{max} ratio was no less than 7, where d_{max} is the maximum particle diameter. More recently, the ASTM standards D6528 and D8296 specify the specimen size requirements for CDSS testing, including a minimum diameter of 45 mm, a minimum height of 12 mm, and a *D/H* ratio higher than 2.5. In addition, *H* must be at least 10 times the maximum particle diameter.

Another critical factor that can affect the liquefaction resistance of clean sand is the loading frequency (*f*). The *f* range of real earthquake motion varies widely, typically from a few hertz to 15 Hz (Silva 1988, Hussain and Sachan 2020a). However, laboratory studies have been conducted at lower *f* values [e.g., 0.03 Hz (Fuenkajorn and Phueakphum 2010), 0.05 Hz (Gratchev *et al.* 2007), 0.1 Hz (Sonmezer 2019a, b, Hussain and Sachan 2022), and 0.2 Hz (Ghionna and Porcino 2006)] to improve testing control and error correction in loading imposition, axial and shear strain, and excess pore water pressure measurement. Therefore, *f* is an essential factor to consider in laboratory tests (Hussain and Sachan 2020b).

*Corresponding author, Ph.D. Student
E-mail: lam.trandongkiem@uah.edu.vn
[a]Professor
E-mail: sungpark@knu.ac.kr
[b]Professor
E-mail: dolee@knu.ac.kr

http://www.techno-press.org/?journal=gae&subpage=7
ISSN: 2005-307X (Print), 2092-6219 (Online)

Since the first research of Peacock and Seed (1968) on the effect of *f* on the liquefaction resistance of sand, there has yet to be a clear consensus on the matter. For example, the CDSS test results of Peacock and Seed (1968) showed only a minor effect on Monterey sand at a relative density of 50% with *f* of 0.17–4 Hz. Other researchers (Lee and Focht 1975, Wong *et al.* 1975, Yoshimi and Oh-oka 1975, Vernese and Lee 1977, Tatsuoka *et al.* 1983, 1986, Polito 1999) reported similar findings. However, Mulilis (1975) observed a fascinating trend in the cyclic triaxial (CTX) tests on loose sand specimens, where sand specimens at a *f* of 0.017 Hz displayed roughly 12% more strength than those at a *f* of 1.0 Hz. Similarly, Dash and Sitharam (2016) found that the cyclic strength of the original Ahmedabad sand declined as *f* increased from 0.1 to 0.5 Hz. In contrast, Lee and Fitton (1969) claimed that *f* increased the number of cycles required to cause liquefaction ($N_{cyc\text{-}liq}$). Nong *et al.* (2020) also observed increased sand liquefaction resistance with *f* in a series of CDSS tests on loose and dense Nakdong River sand, with *f* ranging from 0.05 to 1 Hz. Recent reports by Zhang *et al.* (2019), Zhu *et al.* (2021), and Zeybek (2022) also support this conclusion. Furthermore, Chang *et al.* (1982) reported that the influence of *f* on the liquefaction potential of Monterey No. 0 sand specimens with medium relative density was insignificant at *f* below 0.01 Hz but became significant at *f* above 0.01 Hz. This result was confirmed in a recent study by Park *et al.* (2023), who conducted a series of CDSS tests and found that the effect of *f* became significant at a frequency of 0.1 Hz. Therefore, the effect of *f* on the liquefaction potential of sandy soils still has many uncertainties and requires further exploration in conjunction with other influential factors.

This study aims to investigate the effects of *f* and *D/H* ratio on the cyclic behavior and liquefaction potential of Jumunjin sand by conducting a series of undrained CDSS tests. The dry clean sand specimens with different *D/H* ratios (3.63, 3.21, 2.82, and 2.54) and a wide range of *f* values (0.05, 0.10, and 0.20 Hz) were examined. This study presents valuable insights into the effects of *D/H* ratio and *f* on the liquefaction resistance of sand and proposes a new correction factor to account for their effects. These findings can enhance the design and analysis of structures constructed on or near sandy soils and better understand sandy soil behavior under cyclic loading.

2. Material and testing program

2.1 Material

The material used in this study was Jumunjin sand, a prevalent type of sandy soil predominantly found in South Korea. The properties of this material are presented in Table 1, offering a comprehensive overview of its characteristics. The minimum and maximum void ratios of the sand were 0.571 and 0.903 (using JIS A 1224 (2020)), respectively. To understand its physical properties, its particle size distribution curve (according to (ASTM D 422-63, 2014)) is presented in Fig. 1, providing valuable insights into the distribution of particle sizes within the sand. The type of Jumunjin sand used in the paper is characterized as sand with 100% particle size within the range of 2-0.075 mm. This sand has been categorized as SP according to the Unified Soil Classification System.

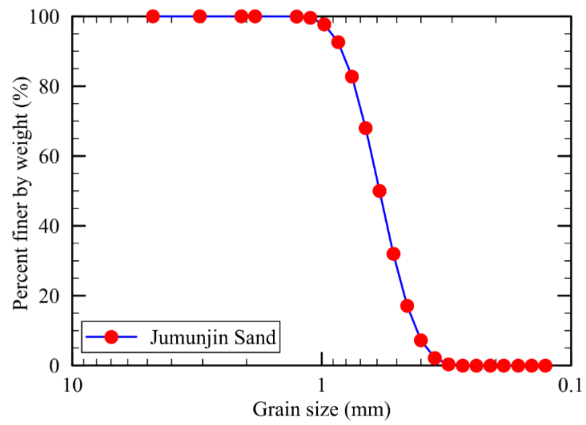

Fig. 1 Grain size distribution curve of Jumunjin sand.

Table 1 Material properties of Jumunjin sand

Type	D_{10} (mm)	D_{30} (mm)	D_{60} (mm)	C_u	C_c	e_{max}	e_{min}	G_s
Jumunjin	0.415	0.508	0.631	1.52	0.98	0.903	0.571	2.65

2.2 CDSS tests and specimen preparation

The CDSS tests were conducted using Geocomp Systems, which has been used in recent studies (Nong *et al.* 2020, 2021, Park *et al.* 2023). Stacked rigid rings were used to attain lateral confinement. The cyclic test was conducted on cylindrical sand specimens with an initial diameter of 63.5 mm. The *H* of these specimens varied between 17.5, 20.0, 22.5, and 25.0 mm to cover *D/H* ratios of 3.63, 3.18, 2.82, and 2.54. In the case of loose sand, a total amount of dry sand was poured into a mold once through a funnel. Conversely, for dense sand, the specimen was divided into four equal layers, each with an identical amount of dry sand. By employing the dry deposition method applied by Lade and Yamamuro (1997) and Yamamuro and Lade (1997), each layer was poured into the mold and then slightly compacted through trial-and-error adjustments. The relative densities were determined based on the mass of the dry sand and the specimen's volume after consolidation, which approximated to 40% and 80% for loose and dense sand, respectively. Moreover, it has been shown that both dry and saturated clean sand exhibit comparative cyclic behavior (Monkul *et al*. 2015); therefore, in this study, all CDSS tests were conducted using dry specimens (Sonmezer *et al*. 2022).

2.3 Testing program and liquefaction criteria

Following the reconstitution stage, all specimens were consolidated under an initial vertical effective stress (σ_{v0}') of 100 kPa. After consolidating, uniform sinusoidal cyclic shear stress with various *f* values (*f* = 0.05, 0.10, and 0.20 Hz) and a wide range of cyclic stress ratios (i.e., $CSR=\tau_{cyc}/$

Table 2 Summary of CDSS tests for investigating the effects of *D/H* ratio and *f*

D_{rc} (%)	*H* (mm)	*f* (Hz)	*CSR*
40, 80	17.5, 20.0, 22.5, and 25.0	0.05, 0.1, and 0.2	0.04, 0.06, 0.08, 0.10, and 0.12

*D_{rc}: The relative density after consolidation

Table 3 Summary of CDSS test results

IDs	*H (mm)*	*D/H*	*f*	CRR_{15}	
				Loose	*Dense*
H175f005			0.05	0.052	0.061
H175f010	17.5	3.63	0.10	0.056	0.066
H175f020			0.20	0.060	0.073
H200f005			0.05	0.060	0.068
H200f010	20.0	3.18	0.10	0.060	0.073
H200f020			0.20	0.067	0.084
H225f005			0.05	0.063	0.077
H225f010	22.5	2.82	0.10	0.071	0.080
H225f020			0.20	0.077	0.092
H250f005			0.05	0.073	0.088
H250f010	25.0	2.54	0.10	0.080	0.092
H250f020			0.20	0.083	0.119

* *ID Hxfy*: denoted the specimen has the *H* of *x* and was subject to the cyclic loading phase with a *f* of *y* Hz

σ_{v0}') was applied to the specimens. The description of the testing program can be found in Table 2. To simulate the undrained condition, a constant-volume shear test was conducted, which involved adjusting the vertical effective stress (σ_v') automatically to maintain the specimen's volume during the cyclic phase, and the change in σ_v' was equivalent to the excess pore pressure (*EPP*) (Bjerrum and Landva 1966, Dyvik *et al*. 1987, Gujrati *et al*. 2023).

In this study, the definition of liquefaction is based on observing either the *EPP* ratio exceeding 100% or the double cyclic shear strain (γ_{cyc}) exceeding 7.5% (NRC 1985, Ishihara 1993), whichever occurs first. The number of cycles required to cause liquefaction is represented by $N_{cyc\text{-}liq}$, and the cyclic resistance ratio (CRR_{15}) signifies liquefaction occurring within 15 cycles, corresponding to an earthquake magnitude (M) of 7.5 (Seed *et al.* 1975, Nong *et al.* 2021, Tran *et al*. 2024).

3. Results and discussion

3.1 Test results

The results of the CDSS tests conducted in this study are summarized in Table 3, providing a comprehensive summary of the test ID, *H*, *D/H* ratio, *f*, and CRR_{15} of the specimens for loose and dense sand, respectively.

3.2 Typical stress-controlled undrained CDSS tests

Figs. 2 and 3 depict the undrained cyclic behavior of

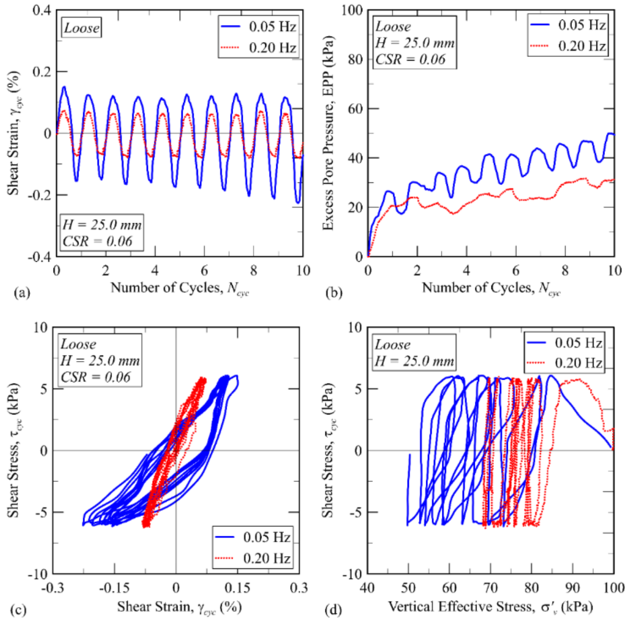

Fig. 2 Typical results of the stress-controlled CDSS test affected by loading frequency (*f* = 0.05 and 0.20 Hz) in the case of loose sand with a *H* of 25.0 mm and a CSR of 0.06: (a) γ_{cyc}–N_{cyc} curve, (b) *EPP*–N_{cyc} curve, (c) τ_{cyc}–γ_{cyc} curve and (d) τ_{cyc}–σ_v' curve

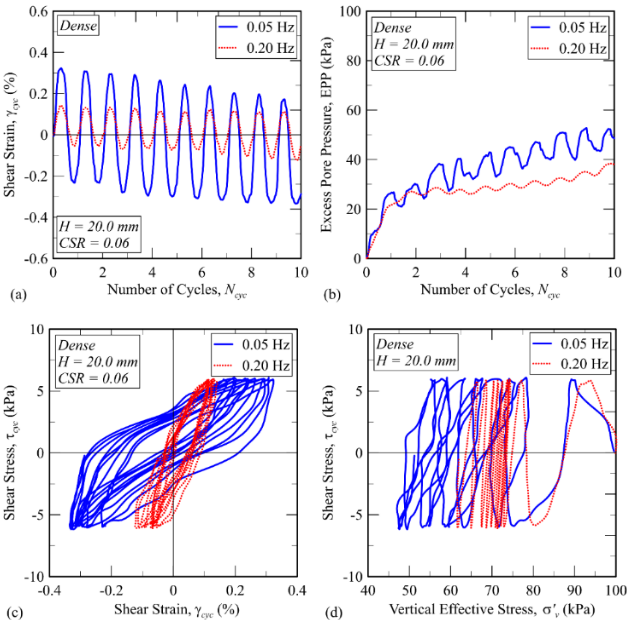

Fig. 3 Typical results of the stress-controlled CDSS test affected by loading frequency (*f* = 0.05 and 0.20 Hz) in the case of dense sand with a *H* of 20.0 mm and a CSR of 0.06: (a) γ_{cyc}–N_{cyc} curve, (b) *EPP*–N_{cyc} curve, (c) τ_{cyc}–γ_{cyc} curve and (d) τ_{cyc}–σ_v' curve

Jumunjin sand within the first 10 cycles under *f* values of 0.05 and 0.20 Hz. For the loose sand, the *H* of 25.0 mm was evaluated under stress-controlled conditions with a τ_{cyc} of 6 kPa (i.e., *CSR* = 0.06). The dense sand had the same testing parameters as the loose sand except for the *H*, which was 20.0 mm instead of 25.0 mm.

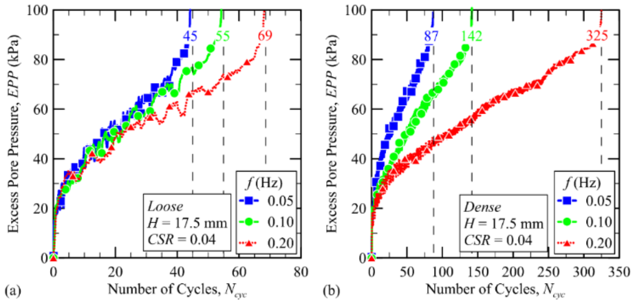

Fig. 4 Effect of f on the *EPP* generation on the Jumunjin sand specimen with an H of 17.5 mm: (a) loose sand and (b) dense sand

In the first 10 cycles, the cyclic shear strain increases with the number of cycles (N_{cyc}) [illustrated in Figs. 2(a)-3(a)] regardless of the f and relative density. Moreover, when the sand specimen was subjected to a higher f, it experienced a lower shear strain starting from the first cycle [Figs. 2(c)-3(c)]. When comparing specimens with the same height, the *EPP* generated are nearly identical in the first cycle. However, beyond the first cycle, the slope of the *EPP* curve is smaller when $f = 0.20$ Hz than when $f = 0.05$ Hz, and this discrepancy increases as N_{cyc} increases.

3.3 Effect of loading frequency

3.3.1 Loading frequency and EPP generation

Fig. 4 illustrates the relationship between *EPP* and N_{cyc} for different f values (0.05, 0.10, and 0.20 Hz), showcasing both the loose and dense specimens with an H of 17.5 mm.

Generally, the *EPP* generation is significant over the first loading cycles regardless of the f and continues to develop slowly as more loading cycles are applied. Furthermore, it is noticeable that f influences the *EPP* generation rate. To be precise, as f increases, there is a considerable decrease in this accumulation rate.

Similar observations were noticed by Nong *et al.* (2020), who stated that when f increases, there is a slow increase in *EPP*, while *CSR* and σ_{v0}' remain constant. As a result of this trend, a higher f necessitates a more significant $N_{cyc\text{-}liq}$ process to take place. A larger f amplitude indicates a higher rate of applying cyclic shear stress onto the specimen. As f increases, the accelerated loading rate prevents the pore pressure from fully developing within the sand specimen (Pandya and Sachan 2022). Consequently, more loading cycles are needed for the specimen to attain the liquefied state. Furthermore, it is noted that the dependence of the *EPP* generation process on f is more pronounced for dense sand. This finding indicates that dense sand is more sensitive to variations in f.

3.3.2 Relationship between loading frequency and the number of cycles to liquefaction

Fig. 5 portrays the effect of f on $N_{cyc\text{-}liq}$ for various *CSR*s for loose sand. At f values of 0.05, 0.10, and 0.20 Hz, the data reveal noteworthy trends for different *CSR*s for each H. For instance, when H = 17.5 mm [Fig. 5(a)], $N_{cyc\text{-}liq}$ increases as f increases when *CSR* = 0.04 (from 45 to 55 and 69 cycles), *CSR* = 0.06 (from 9 to 13 and 14 cycles),

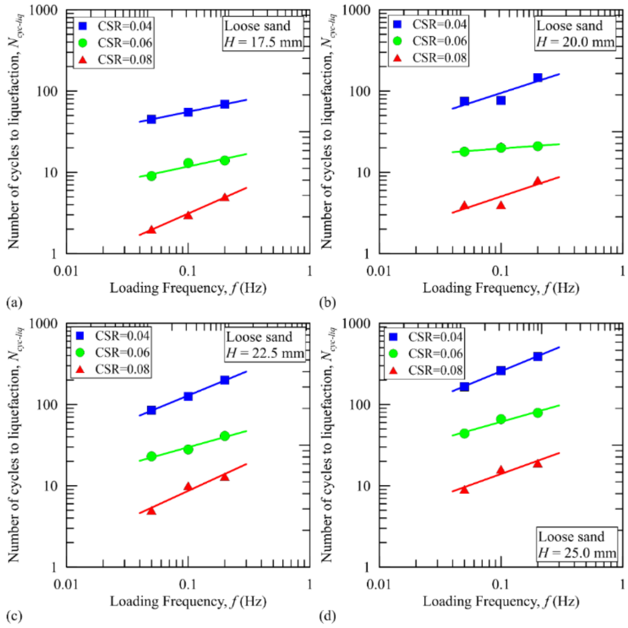

Fig. 5 Effect of f on $N_{cyc\text{-}liq}$ for various *CSR*s for loose sand: (a) H = 17.5 mm, (b) H = 20.0 mm, (c) H = 22.5 mm and (d) H = 25.0 mm

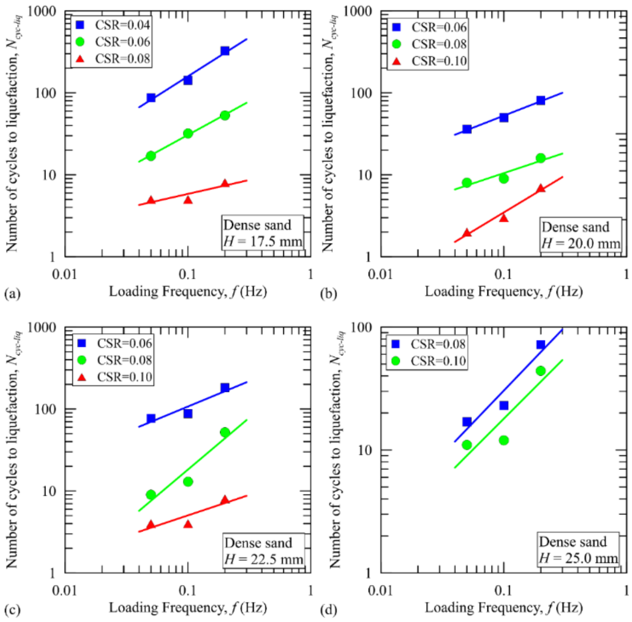

Fig. 6 Effect of f on $N_{cyc\text{-}liq}$ for various *CSR*s for dense sand: (a) H = 17.5 mm, (b) H = 20.0 mm, (c) H = 22.5 mm and (d) H = 25.0 mm

and *CSR* = 0.08 (from 2 to 3 and 5 cycles). Analyzing the data more profoundly reveals a clear trend: As f increases, $N_{cyc\text{-}liq}$ consistently increases regardless of the H or *CSR* values. This observation underscores a strong and direct correlation between f and $N_{cyc\text{-}liq}$, implying that a higher f leads to an increase in $N_{cyc\text{-}liq}$, which is consistent with the understanding stated by Zhu *et al.* (2021).

Fig. 6 presents a resemblance to Fig. 5 but for dense sand. Like in Fig. 5, an increase in f from 0.05 to 0.20 leads to an increase in $N_{cyc\text{-}liq}$ for different *CSR*s for each H. For

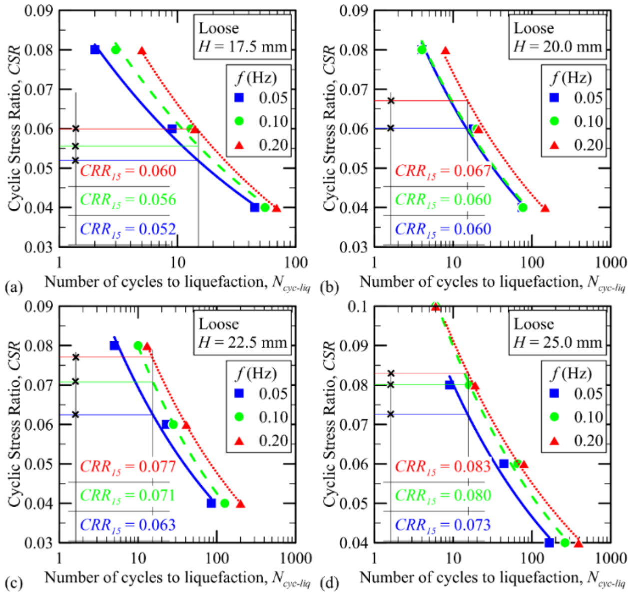

Fig. 7 Cyclic resistance curves of the loose sand in the CDSS tests with various *f* and *H*: (a) *H* = 17.5 mm, (b) *H* = 20.0 mm, (c) *H* = 22.5 mm and (d) *H* = 25.0 mm

instance, when *H* = 17.5 mm [Fig. 6(a)], as *f* increases, $N_{cyc\text{-}liq}$ exhibits an increasing trend when *CSR* = 0.04 (from 87 to 142 and 325 cycles), *CSR* = 0.06 (from 17 to 32 and 53 cycles), and *CSR* = 0.08 (from 5 to 5 and 8 cycles).

From the data presented in Figs. 5 and 6, the relationship between $N_{cyc\text{-}liq}$ and *f* can be depicted using an exponential equation as follows

$$N_{cyc-liq} = c_1 \times f^{c_2} \quad (1)$$

where c_1 and c_2 are coefficients, which can be affected by factors such as the *H* or *D/H* ratio, the relative density, and the *CSR*.

3.3.3 Loading frequency and liquefaction resistance of sand

The liquefaction resistance of sandy soil (i.e., CRR_{15}) is determined based on the cyclic resistance curves of the loose and dense sand. The trend curves presented in Figs. 7 and 8 indicates a functional relationship [Eq. (2)], which has been documented in previous literature (Saxena *et al.* 1988, Boulanger and Idriss 2004, Park and Kim 2013)

$$CSR = c_3 \times N_{cyc-liq}{}^{c_4} \quad (2)$$

where c_3 and c_4 are coefficients, which can be affected by various factors such as the properties of soil, initial state or relative density, initial stress state, *f*, specimen size, and specimen preparation method (Lee and Fitton 1969, Tatsuoka *et al.* 1986, Hird and Hassona 1990, Manmatharajan 2022).

Fig. 9 presents the relationship between CRR_{15} and *f* for different *H* values for two relative densities. There is a positive correlation between CRR_{15} and *f*, where CRR_{15} increases as *f* ranges from 0.05 to 0.20 Hz, which is compatible with most recent studies in Table 2. Notably, in the case of loose sand, the CRR_{15} values vary within the ranges of 0.052–0.06, 0.06–0.067, 0.063–0.077, and 0.073–

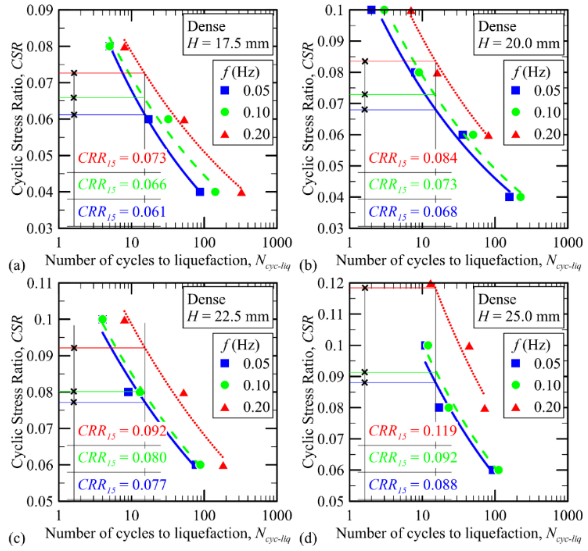

Fig. 8 Cyclic resistance curves of the dense sand in the CDSS tests with various *f* and *H*: (a) *H* = 17.5 mm, (b) *H* = 20.0 mm, (c) *H* = 22.5 mm and (d) *H* = 25.0 mm

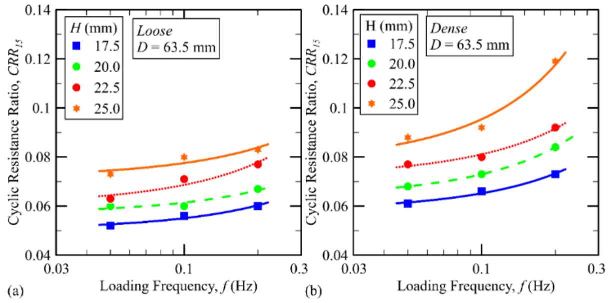

Fig. 9 Effect of *f* on CRR_{15} with various *H*s: (a) Loose sand and (b) dense sand

0.083 when *f* ranges from 0.05 to 0.20 Hz. Additionally, an increase in *f* results in an approximate increase in CRR_{15} of 15%, 12%, 22%, and 14% as *H* varies from 17.5 to 25.0 mm.

Similarly, in the case of dense sand, as *H* ranges from 17.5 to 25.0 mm and *f* increases from 0.05 to 0.20 Hz, CRR_{15} experiences respective increases of 20%, 24%, 19%, and 35%. These findings indicate that the influence of *f* on CRR_{15} is more pronounced in dense sand than in loose sand and this relation depends on *H*. This phenomenon can be explained based on the generation of *EPP* and the accumulation of shear strain during cyclic loading. Specifically, when subjecting a sand specimen to higher *f*, the time available for *EPP* generation diminishes, reducing the accumulation of shear strain. This observation aligns with that by Nong and Park (2021), which noted that experiments conducted at lower *f* resulted in a more considerable volumetric strain accumulation. Normandeau and Zimmie (1991) further validated that within the *f* range of 0.2–0.025 Hz, *f* and the accumulated deformation are inversely proportional.

According to the data provided in Fig. 9, the correlation between CRR_{15} and *f* can be illustrated using a regression equation as follows

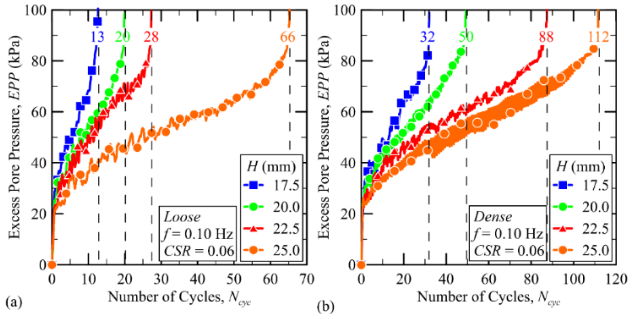

Fig. 10 Effect of *H* on the *EPP* generation on the Jumunjin sand specimen with a *f* of 0.10 Hz: (a) Loose sand and (b) dense sand

$$CRR_{15} = c_5 \times e^{f \times c_6} \tag{3}$$

where c_5 and c_6 are coefficients, which can be affected by the *H* or *D/H* ratio and the relative density.

3.4 Effect of specimen height

3.4.1 Specimen height and EPP generation

The effect of *H* on the *EPP* generation on the loose and dense sand is illustrated in Fig. 10. The data were collected from the CDSS tests, which were conducted at a *f* of 0.10 Hz while the *H* was varied: 17.5, 20.0, 22.5, and 25.0 mm. Upon analysis of Fig. 10, it is evident that the *EPP* generation is significant during the first loading cycles. This phenomenon was observed regardless of the *H* or relative density. As the loading cycles continued to be applied, the rate at which the *EPP* increased decelerated. This indicates that the pore pressure accumulation process exhibits a diminishing rate as the cyclic loading is applied continuously. It is discernible from the results that greater *H* led to a substantial reduction in the rate of *EPP* buildup. This pattern remained consistent for the loose and dense sand, indicating that *H* plays a crucial role in governing *EPP* generation. Carroll (1979) also examined this aspect by performing CDSS tests on a clay specimen with a cross-sectional area of 17.8 cm^2 and varying *H* values (10.9, 17.0, 18.4, and 24.0 mm). The investigation found that within the range of studied *H* values, *EPP* generation generally decreased as *H* increased.

3.4.2 Relationship between specimen height and the number of cycles to liquefaction

The cross curves from Figs. 5 and 6 are plotted in Figs. 11 and 12, respectively, to demonstrate the effect of the change in *H* on $N_{cyc\text{-}liq}$ for loose and dense sand, respectively.

Fig. 11 encompasses three distinct subplots, with each corresponding to *f* = 0.05 Hz [Fig. 11(a)], *f* = 0.10 Hz [Fig. 11(b)], and *f* = 0.20 Hz [Fig. 11(c)]. Likewise, Fig. 12 incorporates two subplots, with each corresponding to *f* = 0.05 Hz [Fig. 12(a)] and *f* = 0.10 Hz [Fig. 12(b)]. The results clearly show that *H* also has a substantial influence on $N_{cyc\text{-}liq}$. As *H* varies, $N_{cyc\text{-}liq}$ demonstrates discernible patterns across different CSRs for each *f*. Higher *H* generally corresponds to increased $N_{cyc\text{-}liq}$, indicating

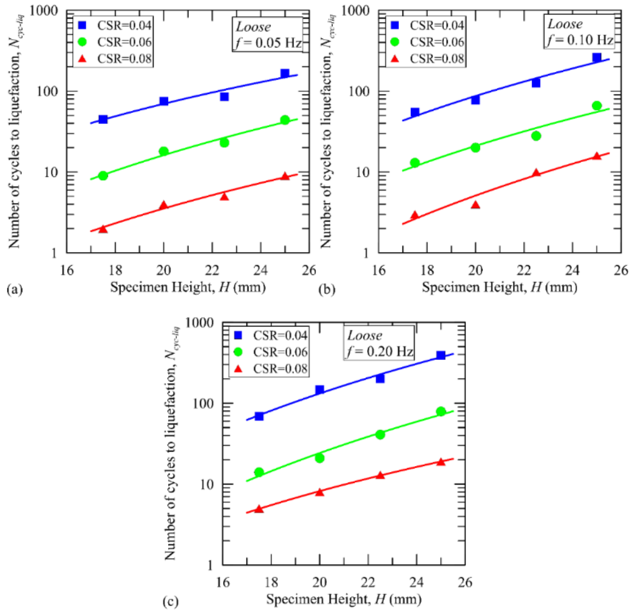

Fig. 11 Effect of *H* on $N_{cyc\text{-}liq}$ for various *CSR*s for loose sand with different *f*: (a) *f* = 0.05 Hz, (b) *f* = 0.10 Hz and (c) *f* = 0.20 Hz

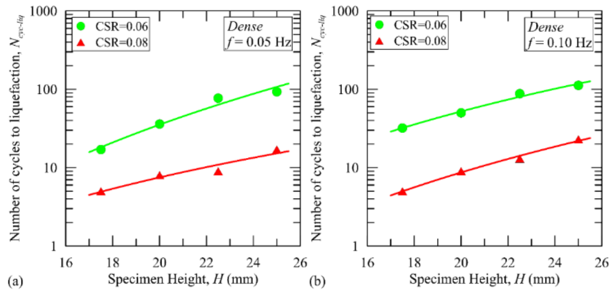

Fig. 12 Effect of *H* on $N_{cyc\text{-}liq}$ for various *CSR*s for dense sand with different *f*: (a) *f* = 0.05 Hz and (b) *f* = 0.10 Hz

enhanced liquefaction resistance. This trend remains consistent across all *f* values and relative densities.

The correction between $N_{cyc\text{-}liq}$ and *H* can be represented by an exponential equation as follows

$$N_{cyc-liq} = c_7 \times e^{H \times c_8} \tag{4}$$

where c_7 and c_8 are coefficients, which can be influenced by factors such as the relative density, *f*, and the *CSR*.

3.4.3 Specimen Height and Liquefaction Resistance of Sand

To provide a more detailed analysis regarding the influence of *H* (or *D/H* ratio) on the liquefaction resistance of sand, Figs. 13 and 14 depict the variation in CRR_{15} concerning *H* and the *D/H* ratio, respectively, for each *f* ranging from 0.05 to 0.20 Hz.

In general, within the range of *f*, increasing the *H* significantly enhances CRR_{15} (Fig. 13). In other words, when the *D/H* ratio increases, the sand specimen's liquefaction resistance diminishes (Fig. 14). Specifically, as *f* varies from 0.05 to 0.20 Hz and *H* increases from 17.5 to 25.0 mm, the liquefaction resistance of the loose sand exhibits an average increase of 41% [40%, 43%, and 38%

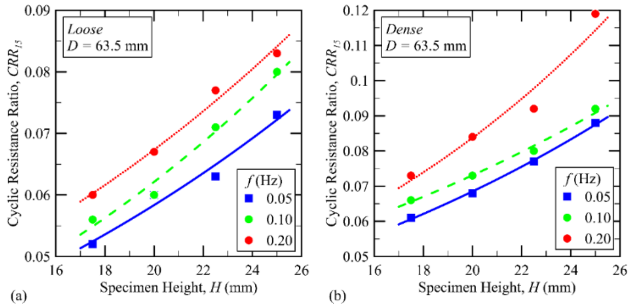

Fig. 13 Effect of H on CRR_{15} with various f: (a) Loose sand and (b) dense sand

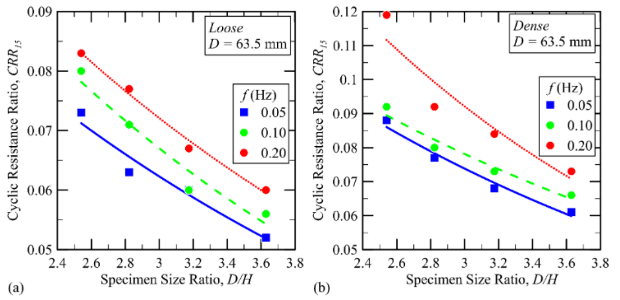

Fig. 14 Effect of D/H on CRR_{15} with various f: (a) Loose sand and (b) dense sand.

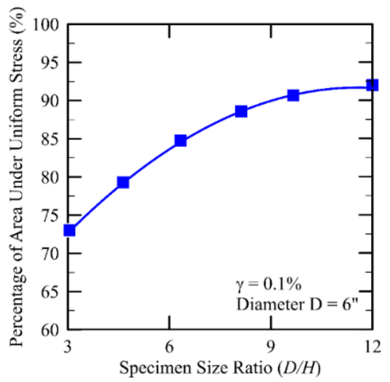

Fig. 15 Ratio of the area subjected to a uniform shear stress to the total area of the specimen by (Amer *et al.* 1987).

when f = 0.05, 0.10, and 0.20 Hz, respectively; Figure 13(a)], while that of the dense sand shows an approximate increase of 50% [44%, 39%, and 63% when f = 0.05, 0.10, and 0.20 Hz, respectively; Fig. 13(b)]. These findings indicate that the influence of H on CRR_{15} is more pronounced in dense sand than in loose sand.

Specimen size alteration can influence stress and strain distributions during simple shear (Amer *et al.* 1987, Wang and Gutierrez 2010, Chang *et al.* 2016, Amipour *et al.* 2022). Despite the incapacity of CDSS devices to replicate ideal conditions fully for simple shear (Bjerrum and Landva 1966, Budhu 1984), certain studies have revealed that approximately 70% to 80% of the soil specimen's cross-sectional area encounters uniform stress and strain (Doherty and Fahey 2011, Chang *et al*. 2016, Amipour *et al*. 2022). Furthermore, this percentage increases as the height of the soil specimen decreases (Amer *et al.* 1987b, Amipour *et al.* 2022). In other words, the nonuniformity in the shear stress distribution intensifies with the heightened H (i.e., the D/H ratio decreases) (Fig. 15).

As a result, the increase in the D/H ratio directly leads to a decrease in both shear modulus and damping ratio (Kovacs and Leo 1981, Amer *et al.* 1987). This subsequently leads to the diminished liquefaction resistance of the specimen.

Table 4 Summary of *NCRR* values

D_{rc} (%)	H (mm)	D/H	Normalized Cyclic Resistance Ratio (NCRR) f = 0.05 Hz	f = 0.10 Hz	f = 0.20 Hz
40	17.5	3.63	0.712	0.700	0.723
	20.0	3.18	0.822	0.750	0.807
	22.5	2.82	0.863	0.888	0.928
	25.0	2.54	1.000	1.000	1.000
80	17.5	3.63	0.693	0.717	0.613
	20.0	3.18	0.773	0.793	0.706
	22.5	2.82	0.875	0.870	0.773
	25.0	2.54	1.000	1.000	1.000

3.5 Cyclic resistance ratio (NCRR), loading frequency, and specimen size ratio

As previously mentioned, the results indicate that the influence of f (increasing about 20%) on CRR_{15} is less significant compared to the effect of D/H (increasing about 45%). Therefore, the *NCRR* based on the influence of the D/H ratio is defined in the following equation and utilized for a more in-depth analysis

$$NCRR = \frac{CRR_{15}^{H-f}}{CRR_{15}^{H=25-f}} \quad (5)$$

where CRR_{15}^{H-f} is the CRR_{15} of the specimen with a height of H and $CRR_{15}^{H=25-f}$ is the CRR_{15} of the 25 mm high specimen with a specimen in the same f series. The *NCRR* was calculated and is summarized in Table 4.

The plot in Fig. 16 illustrates the relationship between the *NCRR* and the D/H ratio. Generally, the *NCRR* decreases as the D/H ratio increases. This study's data analysis revealed a linear relationship between the *NCRR* and the D/H ratio, considering three f values and two relative densities. The figure indicates that the influence of f on the *NCRR* variation is relatively negligible and can be disregarded for loose sand. However, the f for dense sand has a more substantial effect, which also depends on the D/H ratio. Specifically, when the D/H ratio is 2.82, the *NCRR* experiences a change of approximately 10%. As the D/H ratio increases to 3.63, the corresponding change in the *NCRR* ranges from around 14.5%. These effects were observed within the f range of 0.05–0.20 Hz.

Statistical analysis was performed on the data obtained from Table 4. Eight cases were examined, and regression equations were derived (Eq. (6)) and the value of coefficients a and b are presented in Table 5. Each case was investigated using specific parameters, including a D of

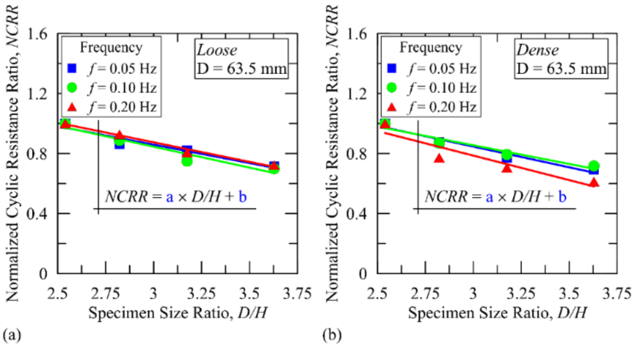

Fig. 16 Relationship between the *NCRR* and the *D/H* ratio with various *f*: (a) Loose sand and (b) dense sand

Table 5 Values of *a* and *b* in regression equations between the *NCRR* and the *D/H* ratio

D_{rc} (%)	*f* (Hz)	*a*	*b*	R^2
40	0.05	-0.2457	1.597	0.942
	0.10	-0.2792	1.684	0.931
	0.20	-0.2607	1.657	0.985
80	0.05	-0.2765	1.676	0.959
	0.10	-0.2491	1.603	0.943
	0.20	-0.3270	1.768	0.869

63.5 mm, the relative density, and a σ_{v0}' of 100 kPa. Table 5 also includes the coefficient of determination (R^2), indicating the goodness of fit for the regression equations.

$$NCRR = a \times (D/H) + b \quad (6)$$

where *a* and *b* are coefficients, which can be influenced by factors such as the relative density, and *f*.

To facilitate calculations, an interpolation formula [Eq. (7)] was established to correlate the *NCRR* and the *D/H* ratio regardless of the *f* and relative density

$$NCRR = -0.273 \times (D/H) + 1.664 \quad (7)$$

where *NCRR* is defined in Eq. (5) and *D/H* is the specimen size ratio. However, it is essential to note that this interpolation formula may yield a lower R^2 of 0.868.

4. Conclusions

This study investigates the effects of *f* and *D/H* ratio on the liquefaction resistance of clean sand. A series of undrained CDSS tests were conducted on Jumunjin sand with two relative densities (D_{rc} = 40% and 80%), different *f* values (*f* = 0.05, 0.10, and 0.20 Hz), and various *D/H* ratios (*D/H* = 3.63, 3.18, 2.82, and 2.54). The cyclic behavior and liquefaction potential of the sand specimens were analyzed, and a correction factor was proposed to account for the effects of *f* and *D/H* ratio. The findings of this study are as follows.

• Both *f* and *H* significantly affect the CRR_{15} and $N_{cyc\text{-}liq}$ of the sand specimens.

• $N_{cyc\text{-}liq}$ increases linearly with *f* for constant vertical stress and CSR, while an increase in *H* leads to higher $N_{cyc\text{-}liq}$ for all *f* values and relative densities.

• There is a positive correlation between CRR_{15} and *f*, indicating that higher *f* results in higher CRR_{15} values. The influence of *f* on CRR_{15} is more pronounced in dense sand than in loose sand. Additionally, *H* significantly impacts CRR_{15}, with an increase in *H* leading to higher CRR_{15} values.

• The effect of *f* on CRR_{15} is less notable compared to the influence of *H*.

• The relationship between the *NCRR* and the *D/H* ratio was analyzed, showing that the *NCRR* generally decreases as the *D/H* ratio increases. The influence of *f* on the *NCRR* is relatively negligible for loose sand but more substantial for dense sand, depending on the *D/H* ratio.

• An formula $NCRR = -0.273 \times (D/H) + 1.664$ was provided to calculate the *NCRR* based on the *D/H* ratio irrespective of the *f* and relative density, although it may produce a lower R^2 of 0.868.

Acknowledgments

The research described in this paper was financially supported by a National Research Foundation of Korea (NRF) grant funded by the Korean government (MSIT) (No. NRF-2018R1A5A1025137).

References

Amer, M.I., Kovacs, W.D. and Aggour, M.S. (1987b), "Cyclic simple shear size effects", *J. Geotech. Eng.*, **113**(7), 693-707. https://doi.org/10.1061/(ASCE)0733-9410(1987)113:7(693).

Amipour, S., Khashila, M., Bayoumi, A., Karray, M. and Chekired, M. (2022), "Specimens size effect D/H on cyclic behaviour and liquefaction potential of clean sand", *Acta Geotech.*, **17**(5), 2047-2057. https://doi.org/10.1007/s11440-021-01339-x.

ASTM D422-63 (2014), Standard test method for particle-size analysis of soils. Annual Book of ASTM Standards, American Society for Testing and Materials International, West Conshohocken, USA.

Bjerrum, L. and Landva, A. (1966), "Direct simple-shear tests on a Norwegian quick clay", *Géotechnique*, **16**(1), 1-20. https://doi.org/10.1680/geot.1966.16.1.1.

Boulanger, R.W. and Idriss, I.M. (2004), Evaluating the potential for liquefaction or cyclic failure of silts and clays. Citeseer.

Budhu, M. (1984), "Nonuniformities imposed by simple shear apparatus", *Can. Geotech. J.*, **21**(1), 125-137. https://doi.org/10.1139/t84-010.

Carroll, M.D. (1979), Sample Size Effects Using the NGI Direct Simple Shear Apparatus. Air Force Inst Of Tech Wright-Patterson Afb Oh.

Chang, N.Y., Hsieh, N.P., Samuelson, D.L. and Horita, M. (1982), "Effect of frequency on liquefaction potential of saturated monterey No. O sand", *Comput. Method. Exp. Meas.*, (Eds., Keramidas, G.A. and Brebbia,C.A.), 433-446. Berlin, Heidelberg: Springer.

Chang, W.J., Phantachang, T. and Ieong, W.M. (2016), "Evaluation of size and boundary effects in simple shear tests with distinct element modeling", *J. Geoengin.*, **11**(3), 133-142.

https://doi.org/10.6310/jog.2016.11(3).3.

Dash, H.K. and Sitharam, T.G. (2016), "Effect of frequency of cyclic loading on liquefaction and dynamic properties of saturated sand", *Int. J. Geotech. Eng*., **10**(5), 487-492. https://doi.org/10.1080/19386362.2016.1171951.

Doherty, J. and Fahey, M. (2011), "Three-dimensional finite element analysis of the direct simple shear test", *Comput. Geotech*., **38**(7), 917-924. https://doi.org/10.1016/j.compgeo.2011.05.005.

Dyvik, R., Berre, T., Lacasse, S. and Raadim, B. (1987), "Comparison of truly undrained and constant volume direct simple shear tests", *Geotechnique*, **37**(1), 3-10. https://doi.org/10.1680/geot.1987.37.1.3.

Fuenkajorn, K. and Phueakphum, D. (2010), "Effects of cyclic loading on mechanical properties of Maha Sarakham salt", *Eng. Geol*., **112**(1-4), 43-52. https://doi.org/10.1016/j.enggeo.2010.01.002.

Ghionna, V.N. and Porcino, D. (2006), "Liquefaction resistance of undisturbed and reconstituted samples of a natural coarse sand from undrained cyclic triaxial tests", *J. Geotech. Geoenviron. Eng*., **132**(2), 194-202. https://doi.org/10.1061/(ASCE)1090-0241(2006)132:2(194).

Gratchev, I.B., Sassa, K., Osipov, V.I., Fukuoka, H. and Wang, G. (2007), "Undrained cyclic behavior of bentonite–sand mixtures and factors affecting it", *Geotech. Geol. Eng*., **25**(3), 349. https://doi.org/10.1007/s10706-006-9115-2.

Gujrati, S., Hussain, M. and Sachan, A. (2023), "Liquefaction susceptibility of cohesionless soils under monotonic compression and cyclic simple shear loading at drained/undrained/partially drained modes", *Transp. Infrastruct. Geotechnol*., **10**, 391-423. https://doi.org/10.1007/s40515-022-00226-6.

Hird, C.C. and Hassona, F.A.K. (1990), "Some factors affecting the liquefaction and flow of saturated sands in laboratory tests", *Eng. Geol*., **28**(1-2), 149-170. https://doi.org/10.1016/0013-7952(90)90039-4.

Hussain, M. and Sachan, A. (2022), "Cyclic simple shear behaviour of saturated and moist sandy soils", *Geomech. Geoeng*., **17**, 1762-1785. https://doi.org/10.1080/17486025.2021.1975045.

Hussain, M. and Sachan, A. (2020a), "Dynamic behaviour of Kutch soils under cyclic triaxial and cyclic simple shear testing conditions", *Int. J. Geotech. Eng*., **14**, 902-918. https://doi.org/10.1080/19386362.2019.1608715.

Hussain, M. and Sachan, A. (2020b), "Effect of loading conditions and stress history on cyclic behavior of Kutch soil", *Geomech. Geoeng*., **15**, 233-251. https://doi.org/10.1080/17486025.2019.1635716.

Ishihara, K. (1993), "Liquefaction and flow failure during earthquakes", *Geotechnique*, **43**(3), 351-451. https://doi.org/10.1680/geot.1993.43.3.351.

JIS A 1224 (2020), Test method for minimum and maximum densities of sands. Japanese Standards Association (JSA), Tokyo, Japan.

Kovacs, W.D. and Leo, E. (1981), "Cyclic simple shear of large scale sand samples: effects of diameter to height ratio", *Int. Conf. Recent Adv. Geotech. Earthq. Eng. Soil Dyn*., 897-904.

Lade, P.V. and Yamamuro, J.A. (1997), "Effects of nonplastic fines on static liquefaction of sands", *Can. Geotech. J*., **34**(6), 918-928. National Research Council of Canada. https://doi.org/10.1139/t97-052.

Lee, K. and Fitton, J. (1969), "Factors affecting the cyclic loading strength of soil", *Vib. Eff. Earthq. Soils Found*., https://doi.org/10.1520/STP33637S. Barr Harbor Drive, PO Box C700, West Conshohocken, PA 19428-2959: ASTM International.

Lee, K.L. and Focht, J.A. (1975), "Liquefaction potential at Ekotisk tank in North Sea", *J. Geotech. Eng. Div*., **101**(1), 1-18. American Society of Civil Engineers. https://doi.org/10.1061/AJGEB6.0000138.

Manmatharajan, V. (2022), "Factors affecting liquefaction assessment of granular soils through laboratory testing", PhD Thesis. University of Toronto (Canada).

Monkul, M.M., Gültekin, C., Gülver, M., Akin, Ö. and Eseller-Bayat, E. (2015), "Estimation of liquefaction potential from dry and saturated sandy soils under drained constant volume cyclic simple shear loading", *Soil Dyn. Earthq. Eng*., **75**, 27-36. https://doi.org/10.1016/j.soildyn.2015.03.019.

Mulilis, J.P. (1975), "The effects of method of sample preparation on the cyclic stress-strain behaviour of sands", Tech. Rep. Univ Calif. Berkeley, 75.

Nong, Z., Park, S.S., Jeong, S.W. and Lee, D.E. (2020), "Effect of cyclic loading frequency on liquefaction prediction of sand", *Appl. Sci. Switz*., **10**(13). https://doi.org/10.3390/app10134502.

Nong, Z.Z., Park, S.S. and Lee, D.E. (2021), "Comparison of sand liquefaction in cyclic triaxial and simple shear tests", *Soils Found*., **61**(4), 1071-1085. The Japanese Geotechnical Society. https://doi.org/10.1016/j.sandf.2021.05.002.

Nong, Z.Z. and Park, S.S. (2021), "Effect of loading frequency on volumetric strain accumulation and stiffness improvement in sand under drained cyclic direct simple shear tests", *J. Geotech. Geoenviron. Eng*., **147**(12). https://doi.org/10.1061/(asce)gt.1943-5606.0002706.

Normandeau, D.E. and Zimmie, T.F. (1991), "The effect of frequency of cyclic loading on earth structures and foundation soils", University of Missouri–Rolla.

NRC (1985), "Liquefaction of soils during earthquakes", Comm. Earthq. Eng. National Academy Press.

Pandya, S. and Sachan, A. (2022), "Effect of frequency and amplitude on dynamic behaviour, stiffness degradation and energy dissipation of saturated cohesive soil", *Geomech. Geoeng*., **17**(1), 30-44. https://doi.org/10.1080/17486025.2019.1680885.

Park, S.S. and Kim, Y.S. (2013), "Liquefaction resistance of sands containing plastic fines with different plasticity", *J. Geotech. Geoenviron. Eng*., **139**(5), 825-830. https://doi.org/10.1061/(ASCE)GT.1943-5606.0000806.

Park, S.S., Tran, D.K.L., Nguyen, T.N., Woo, S.W. and Sung, H.Y. (2023), "Effect of loading frequency on the liquefaction resistance of poorly graded sand", Adv. Geospatial Technol. Min. Earth Sci. Sel. Pap. 2nd Int. Conf. Geo-Spat. Technol. Earth Resour. 2022.

Peacock, W.H. and Seed, H.B. (1968), "Sand liquefaction under cyclic loading simple shear conditions", *J. Soil Mech. Found. Div*., **94**(3), 689-708. American Society of Civil Engineers. https://doi.org/10.1061/JSFEAQ.0001135.

Polito, C. (1999), "The effects of non-plastic and plastic fines on the liquefaction of sandy soils", PHD TheisVirginia Tech, (December): 274.

Saxena, S.K., Reddy, K.R. and Avramidis, A.S. (1988), "Liquefaction resistance of artificially cemented sand", *J. Geotech. Eng*., **114**(12), 1395-1413. https://doi.org/10.1061/(ASCE)0733-9410(1988)114:12(1395).

Seed, H.B., Idriss, I.M., Makdisi, F. and Banerjee, N. (1975), "Representation of irregular stress time histories by equivalent uniform stress series in liquefaction analyses", Report No. EERC 75-29. Earthq. Eng. Res. Cent. Univ. Calif. Berkeley.

Shen, C.K., Herrmann, L.R. and Sadigh, K. (1978), "An analysis of NGI simple shear apparatus for cyclic soil testing", *Dyn. Geotech. Test*., 148-162. ASTM International.

Silva, W. (1988), Soil response to earthquake ground motion: Final report. Woodward-Clyde Consultants, Walnut Creek, CA (USA).

Sonmezer, Y.B. (2019a), "Investigation of the liquefaction potential of fiber-reinforced sand", *Geomech. Eng.*, **18**(5), 503-513. https://doi.org/10.12989/gae.2019.18.5.503.

Sonmezer, Y.B. (2019b), "Energy-based evaluation of liquefaction potential of uniform sands", *Geomech. Eng.*, **17**(2), 145-156. https://doi.org/10.12989/gae.2019.17.2.145

Sonmezer, Y.B., Kayabali, K., Beyaz, T. and Fener, M. (2022), "Influence of grain size ratio and silt content on the liquefaction potentials of silty sands", *Geomech. Eng.*, **31**(2), 167-181. https://doi.org/10.12989/gae.2022.31.2.167.

Tatsuoka, F., Maeda, S., Fujii, S. and Yamada, S. (1983), "Cyclic undrained strengths of saturated sand under random and uniform loading and their relation", Bull ERS Inst. Ind. Sci. Univ Tokyo, **16**, 11-31.

Tatsuoka, F., Toki, S., Miura, S., Kato, H., Okamoto, M., Yamada, S., Yasuda, S. and Tanizawa, F. (1986), "Some factors affecting cyclic undrained triaxial strength of sand", *Soil Found.*, **26**(3), 99-116. https://doi.org/10.3208/sandf1972.26.3_99.

Tran, D.K.L., Park, S.S., Nguyen, T.N., Park, J.H., Sung, H.Y., Son, J.H. and Hwang, K.B. (2024a), "Effect of non-plastic fines content on the pore pressure generation of sand-silt mixture under strain-controlled CDSS test", *J. Earthq. Eng. Soc. Korea*, **28**, 33-39. https://doi.org/10.5000/EESK.2024.28.1.033

Tran, D.K.L., Woo, S.W., Lee, S.D., Nguyen, N.N. and Park, S.S. (2024b), "Couple effect of loading frequency and uniformity coefficient on the liquefaction resistance of sand", (Eds., Reddy, J.N., Wang, C.M., Luong, V.H. and Le, A.T.), *Proceedings of the 3rd International Conference on Sustainable Civil Engineering and Architecture*, Lecture Notes in Civil Engineering. Springer Nature Singapore, Singapore, 1085-1091. https://doi.org/10.1007/978-981-99-7434-4_114.

Vernese, F.J. and Lee, K.L. (1977), Effect of frictionless caps and bases in the cyclic triaxial test. Department of Defense, Department of the Army, Corps of Engineers, Waterways….

Wang, J. and Gutierrez, M. (2010), "Discrete element simulations of direct shear specimen scale effects", *Géotechnique*, **60**(5), 395-409. https://doi.org/10.1680/geot.2010.60.5.395.

Wong, R.T., Seed, H.B. and Chan, C.K. (1975), "Cyclic loading liquefaction of gravelly soils", *J. Geotech. Eng. Div.*, **101**(6), 571-583. https://doi.org/10.1061/AJGEB6.0000174.

Yamamuro, J.A. and Lade, P.V. (1997), "Static liquefaction of very loose sands", *Can. Geotech. J.*, **34**(6), 905-917. https://doi.org/10.1139/t97-057.

Yoshimi, Y. and Oh-oka, H. (1975), "Influence of degree of shear stress reversal on the liquefaction potential of saturated sand", *Soils Found.*, **15**(3), 27-40. https://doi.org/10.3208/sandf1972.15.3_27.

Zeybek, A. (2022), "Stress-controlled dynamic triaxial experiments to examine the liquefaction response of clean sand", *Bitlis Eren Üniversitesi Fen Bilim. Derg.*, **11**(2), 669-680.

Zhang, J., Cao, J. and Huang, S. (2019), "Experimental study on the effects of initial shear stress and vibration frequency on dynamic strength of saturated sands", *Adv. Mater. Sci. Eng.*, 2019. https://doi.org/10.1155/2019/3758527.

Zhu, Z., Zhang, F., Peng, Q., Dupla, J.C., Canou, J., Cumunel, G. and Foerster, E. (2021), "Effect of the loading frequency on the sand liquefaction behaviour in cyclic triaxial tests", *Soil Dyn. Earthq. Eng.*, **147**, 106779. https://doi.org/10.1016/j.soildyn.2021.106779.

CC

Notation

Notation	*Definition*
C_c	The curvature coefficient
CRR_{15}	Cyclic resistance ratio
CSR	Cyclic stress ratio
C_u	The uniformity coefficient
D	Specimen diameter
D/H	Diameter to Height ratios
EPP	Excess pore pressure
f	Loading frequency
H	Specimen height
N_{cyc}	Number of cycles
$N_{cyc\text{-}liq}$	Number of cycles to cause liquefaction
$NCCR$	Normalized cyclic resistance ratio
γ_{cyc}	The double cyclic shear strain
σ_v'	Vertical effective stress
σ_{v0}'	Initial vertical effective stress
τ_{cyc}	Cyclic shear stress